Direct Measurements of Multiple Adhesive Alignments and Unbinding Trajectories between Cadherin Extracellular Domains

S. Sivasankar,* B. Gumbiner,‡ and D. Leckband*†

*Center for Biophysics and Computational Biology, and †Department of Chemical Engineering, University of Illinois at Urbana-Champaign, Urbana, Illinois 61801, and ‡Memorial Sloan-Kettering Cancer Center, New York, New York 10021 USA

ABSTRACT Direct measurements of the interactions between antiparallel, oriented monolayers of the complete extracellular region of C-cadherin demonstrate that, rather than binding in a single unique orientation, the cadherins adhere in three distinct alignments. The strongest adhesion is observed when the opposing extracellular fragments are completely interdigitated. A second adhesive alignment forms when the interdigitated proteins separate by 70 ± 10 Å. A third complex forms at a bilayer separation commensurate with the approximate overlap of cadherin extracellular domains 1 and 2 (CEC1–2). The locations of the energy minima are independent of both the surface density of bound cadherin and the stiffness of the force transducer. Using surface element integration, we show that two flat surfaces that interact through an oscillatory potential will exhibit discrete minima at the same locations in the force profile measured between hemicylinders covered with identical materials. The measured interaction profiles, therefore, reflect the relative separations at which the antiparallel proteins adhere, and are unaffected by the curvature of the underlying substrate. The successive formation and rupture of multiple protein contacts during detachment can explain the observed sluggish unbinding of cadherin monolayers. Velocity–distance profiles, obtained by quantitative video analysis of the unbinding trajectory, exhibit three velocity regimes, the transitions between which coincide with the positions of the adhesive minima. These findings suggest that cadherins undergo multiple stage unbinding, which may function to impede adhesive failure under force.

INTRODUCTION

Classical cadherins constitute a major component of a particular class of intercellular junctions. Cadherins are transmembrane, cell-surface proteins that bind to identical molecules on opposing cells and mediate adhesion in all soft tissue. Besides their role in maintaining the architecture of adult tissue; cadherins are involved in cell–cell recognition and cell sorting during development (Takeichi, 1991, 1993, 1995; Gumbiner, 1996; Yap et al., 1997). Classical cadherins are single-pass transmembrane proteins, and the extracellular (EC) region is composed of five autonomously folding, homologous EC domains (Shapiro et al., 1995), numbered 1 through 5 from the outermost domain. The tandemly arranged EC domains mediate adhesion in a calcium-dependent fashion (Koch et al., 1999; Nagar et al., 1996; Pertz et al., 1999; Pokutta et al., 1994). Atomic level structural information on the cadherin EC region is available only for the first two domains of neural (NCAD) and epithelial cadherins (ECAD). Early domain-swapping studies indicated that the tissue selectivity resides in the N-terminal domain (Nose et al., 1990). Based on the antiparallel contacts observed in the crystal structure of the outermost domain of NCAD (Shapiro et al., 1995) this domain alone was thought to form the adhesive interface (Shapiro et al., 1995; Weis, 1995). From electron micrographs of ECAD pentamers, Pertz and coworkers (Pertz et al., 1999) inferred that binding is between the outer domains. However, the antiparallel contacts were not observed in the crystal structures of ECAD12 and NCAD12 (Nagar et al., 1996; Tamura et al., 1998). The different interdomain contacts observed in four different crystal structures of the outer domains resulted in contradictory models for the cadherin adhesive mechanism (Koch et al., 1999). In addition, although Koch et al. demonstrated, by electron microscopy, the effects of calcium on the rigidity of the EC domain, they were unable to establish the mechanism of *trans* interactions between the proteins.

The hypothesis that cadherin binds by means of homotypic binding between the N-terminal domains alone was tested by direct measurements, with a surface force apparatus, of both the magnitude and the distance dependence of forces between the EC domains of C-cadherin from *Xenopus* (Sivasankar et al., 1999). The force–distance profiles revealed two important aspects of cadherin binding. First, the proteins bound in two distinct adhesive alignments. This differs from the earlier predictions in that there were multiple binding alignments, and neither one involved direct interactions between the amino-terminal domains. Moreover, the strongest bond is between the completely interdigitated, antiparallel ectodomains. Second, the successive rupture of these multiple contacts during protein detachment slows the unbinding velocity (Sivasankar et al., 1999). However, the sluggish unbinding persisted over a distance equivalent to the full range of ectodomain interaction. Thus, the two adhesive minima could account for only part of the region of impeded detachment, and suggested that additional binding interactions might be involved (Sivasankar et al., 1999).

Received for publication 6 June 2000 and in final form 21 December 2000.

Address reprint requests to Deborah E. Leckband, Dept. of Chemical Engineering, University of Illinois at Urbana-Champaign, 114 Roger Adams Lab., Box C-3, 600 S. Mathews Ave., Urbana, IL 61801.

0006-3495/01/04/1758/11 $2.00

This study demonstrates that cadherin can undergo homophilic binding in three distinct adhesive alignments, the positions of which are independent of the protein surface densities and of the value of the force transducer stiffness. The locations of the binding interactions (bonds) in the force–distance profiles identified three distinct adhesive complexes and the relative protein alignments in each. At all protein coverages, both the strong primary and weaker secondary sites of adhesion are at the identical protein alignments as reported previously (Sivasankar et al., 1999). In this paper, we report the presence of a third, previously unidentified bond at a distance comparable to the overlap between domains 1 and 2 (CEC1–2). Numerical calculations were used to determine the effects of geometry on oscillatory, intersurface potentials. They confirm that oscillatory potentials between two flat surfaces give rise to corresponding oscillations in force–distance profiles measured between two crossed cylinders. Finally, quantitative video analysis of the unbinding trajectories show there are three distinct unbinding velocities, and the transitions between the different velocity regimes occur at roughly the same positions as the three measured attractive minima.

MATERIALS AND METHODS

Chemicals

The copper chelating lipid, distearoyl-glycerylether-iminodiacetic acid (DSIDA) was purchased from Northern Lipids (Vancouver, Canada). Distearoyl phosphatidyl choline (DSPC), di-tridecanoyl phosphatidyl choline (DTPC), and dipalmitoyl phosphatidyl ethanolamine (DPPE) were from Avanti Polar Lipids (Alabaster, AL). Hepes and Tris buffers were from Sigma (St. Louis, MO), and all inorganic salts were from Fisher. *N*-hydroxysulfosuccinimide (NHSS) and 1-ethyl-3-(3-dimethylaminopropyl-)carbodiimide (EDAC) were from Molecular Probes (Eugene, OR), and L-Lysine-N^a,N^a-diacetic acid (aminobutyl-NTA) was from Dojindo Molecular Technologies (Gaithersburg, MD). All aqueous solutions were prepared with water purified with a Milli-Q UV plus water purification system (Millipore, Bedford, MA).

Protein purification

CEC1–5 with a six-histidine tag at the C-terminus was purified from the conditioned medium of Chinese hamster ovary cells expressing CEC 1–5 off the pEE14 expression vector (Brieher et al., 1996). The purification protocol involves the separation of the his-tagged cadherin on a nickel chelating column, an ion exchange column, and finally a size exclusion column (Brieher et al., 1996). We followed the published procedures with a few minor changes. First, the protein was eluted from the ion exchange column with a 10–600-mM NaCl gradient in 20 mM Tris and 2 mM $CaCl_2$ at pH 8.0. Second, in the gel filtration step, the protein was eluted with a solution containing 50 mM NaCl, and 2 mM $CaCl_2$ in 20 mM Hepes at pH 7.5. The yield was typically 4–5 mg of CEC1–5 from 1 liter of conditioned medium.

Bead aggregation assay

The cadherin adhesion activity was assayed by monitoring the ability of his-tagged CEC1–5 to aggregate carboxylate-modified microspheres functionalized with aminobutyl-NTA (TechNote #13c, Covalent Coupling Protocols; Bangs Laboratories, Inc., Fishers, IN). The cadherin was bound to the NTA groups on the microsphere surface by its C-terminal polyhistidine tag. Before activating the microspheres with aminobutyl-NTA, the fluorescently dyed carboxyl-modified beads (5 mg of 1.2 μm microspheres) (Bangs Laboratories Inc.) were washed twice in 0.5 ml de-ionized water to remove surfactant. The beads were then pelleted by centrifugation at $1200 \times g$ for 15 min. The supernatant was discarded, and the spheres were resuspended in buffer. To activate the carboxylate groups on the microsphere surface, 38 mg 1-ethyl-3-(3-dimethylaminopropyl)carbodiimide (EDAC) and 7 mg of *N*-hydroxysulfosuccinimide (NHSS) (Molecular Probes) were reacted with the resuspended microspheres for 15 min with continuous mixing. The activated beads were washed twice in 100 mM Hepes buffer at pH 7.5 and resuspended in 0.25 ml of the same buffer. L-Lysine-N^a,N^a-Diacetic acid (aminobutyl-NTA) (10 mg) was added to the bead suspension and reacted for four hours with constant mixing. To quench the coupling reaction and block the hydrophobic surface of the polymer bead, the activated beads were washed and then resuspended in 5 ml of a solution containing 40 mM glycine and 1% w/v cytochrome c, under gentle agitation for 30 min. The microspheres were then washed twice and resuspended in 1 ml of 100 mM Hepes (pH 7.5), and 0.1% w/v cytochrome c. To activate the NTA groups on the microsphere surface before protein immobilization, $NiSO_4$ was added to a final concentration of 20 μM. When purified, cadherin was added to resuspended beads in the ratio of 0.1 μg protein:2.0 μg beads and incubated for 30 min, large bead aggregates were observed with an Olympus epifluorescence microscope. Beads did not aggregate when bovine serum albumin was used as a control.

Preparation of cadherin monolayers

Oriented C-cadherin monolayers were prepared by binding CEC1–5 via its C-terminal polyhistidine tag to lipid monolayers containing DSIDA (Shnek et al., 1994) (Fig. 1) (Northern Lipids). The lipid films contained 100 mol% or 25 mol% DSIDA, which was mixed with DSPC (Avanti Polar Lipids). The DSPC and DSIDA were shown by fluorescence microscopy to be miscible in all proportions. Gel phase lipids were used in these studies because lipids (melting temperature $T_m < T$) and DSIDA were shown to phase separate above ~40 mol% DSIDA. The lipid monolayers were prepared by spreading a chloroform solution of the lipid mixture at the

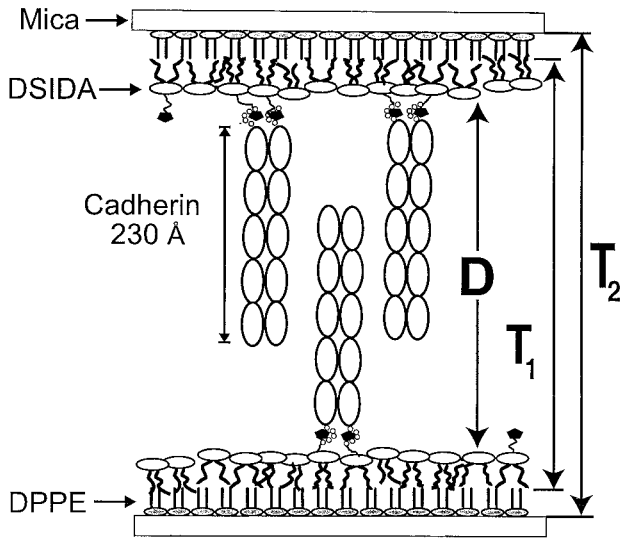

FIGURE 1 Illustration of the immobilized cadherin monolayers used in surface force measurements.

air–water interface of a Langmuir trough (Nima Type 611, Coventry; England). After chloroform evaporation, the monolayer was compressed to an average lipid area of 45 $Å^2$/lipid (DSPC matrix). The aqueous subphase contained 0.25 μM $Cu(NO_3)_2$, 50 mM Tris, 100 mM $NaNO_3$ and 2 mM $Ca(NO_3)_2$ at pH 7.5 and was maintained at 25°C. The monolayer was transferred at constant pressure, by Langmuir–Blodgett deposition, onto a hydrophobic substrate. For surface force measurements, the hydrophobic substrate was a crystalline monolayer of DPPE (43 $Å^2$/lipid) (Avanti Polar Lipids) supported on atomically flat mica (Leckband et al., 1994). For surface plasmon resonance (SPR) measurements, the hydrophobic substrate was a monolayer of 1-octadecanethiol self assembled on a thin gold film. The gold was thermally evaporated onto a glass slide, which was first coated with a 15 Å chromium adhesion layer.

Oriented cadherin monolayers were prepared by transferring the supported lipid bilayers to a small beaker containing approximately 3 μM of CEC1–5 in 3 ml of a solution containing 0.25 μM $Cu(NO_3)_2$, 50 mM Tris, 100 mM $NaNO_3$, and 2 mM $Ca(NO_3)_2$ at pH 7.5. After incubating the DSIDA membranes and protein for an hour, the buffer was exchanged for identical buffer lacking protein. The samples were then gently rinsed with a syringe to remove all nonspecifically adsorbed protein, and the supported bilayer assembly was transferred to the force-measuring apparatus. For SPR measurements, the supported DSIDA monolayers were first mounted in a Teflon flow cell and attached to the sample stage of a home-built SPR instrument (Lavrik and Leckband, 2000). Cadherin monolayers were prepared by incubating the DSIDA lipid monolayers with 9 μM of CEC1–5 in a 1.0-ml solution of 0.25 μM $Cu(NO_3)_2$, 50 mM Tris, 100 mM $NaNO_3$, and 2mM $Ca(NO_3)_2$ at pH 7.5.

Force measurements between a CEC1–5 monolayer and a bare 25 mol% DSIDA membrane served as a control. To prevent the adsorption of adhesive dimers on the bilayer in the control experiments, the protein solution was first desalted using Centricon-30 Concentrators (Amicon, Beverly, MA). The removal of calcium with a 100-fold excess of EDTA disrupted any *trans* cadherin dimers (Brieher et al., 1996). Cadherin was then bound to a 25 mol%-supported DSIDA monolayer in the absence of calcium. Following the transfer of the samples to the surface forces apparatus, calcium addition to the solution, bathing the proteins, reactivated the cadherin. Bead aggregation assays demonstrated that cadherin activity recovered after calcium re-addition.

Characterization of cadherin monolayers

The assembly of the cadherin monolayers was monitored using a home-built SPR Instrument (Lavrik and Leckband, 2000) based on the Kretschmann configuration. A Teflon flow cell housing the DSIDA monolayer was attached to a sample stage, which was rotated by a precision goniometer driven by a stepper motor. A silicon photodiode detector monitored the intensity of a GaAs laser beam reflected off the gold film as a function of the external angle of incidence. Shifts in the resonance angle, at which the reflected light intensity is minimum, were monitored continuously during protein adsorption to the lipid film, and were converted to changes in the optical thickness of the protein monolayer. This was done by fitting the resonance curves to the Fresnel equations for a multilayer film. Initially, we estimated the amount of bound protein from changes in the index of refraction of the adsorbed layer. To do this, we assumed a 230-Å protein film thickness (Nagar et al., 1996; Pokutta et al., 1994; Sivasankar et al., 1999) and a refractive index of 1.44 for the pure protein.

The optical method of quantifying protein coverage is less accurate on account of uncertainties in the refractive index of the protein. Errors in the latter parameter can result in fairly large errors in the determined coverage of thick monomolecular films. For this reason, we quantified the cadherin surface coverage by measuring the amount of ^{125}[I]-labeled cadherin bound to supported bilayers containing different amounts of Cu-IDA-lipid. Radiolabeling and protein quantification were done according to procedures described elsewhere (Vijayendran and Leckband, 1999; Yeung and Leckband, 1997; Yeung et al., 1999).

Surface force measurements

Forces between oriented monolayers of CEC1–5 were measured with the Mark III Surface Forces Apparatus (SFA) (SurForce; Santa Barbara, CA) (Israelachvili and McGuiggan, 1990). The SFA quantifies the force between thin films confined to the surfaces of two, crossed hemicylindrical lenses as a function of their intersurface separation (Israelachvili and Adams, 1978; Israelachvili and McGuiggan, 1990). The net force between the two cylinders, normalized by their geometric average radius, $F_c(D)/R$, is related to the corresponding interaction energy per unit area $E_f(D)$ between two equivalent planar surfaces by the Derjaguin Approximation: $E_f = F_c/2\pi R$. This relationship holds when the separation distance $D \ll R$ (Hunter, 1989; Israelachvili, 1992b).

The intersurface spacing is measured with a resolution of ± 1 Å by multiple beam interferometry (Israelachvili, 1973). The normalized forces are measured with a resolution of 0.1 mN/m from the deflection of a sensitive leaf spring that supports one of the silica lenses (Israelachvili and Adams, 1978). The measurements quantify the total force, integrated over the entire area of contact between the two surfaces, and reflects the interactions of >100,000 proteins. The use of oriented protein monolayers, therefore, insures that the signal is due to a single protein orientation.

All measurements were carried out at 25°C with the samples bathed in a solution of 0.25 μM $Cu(NO_3)_2$, 50 mM Tris, 100 mM $NaNO_3$, and 2 mM $Ca(NO_3)_2$ at pH 7.5. Forces between cadherin monolayers bound to 25 and 40 mol% DSIDA/DTPC lipid bilayers were measured using a spring stiffness of 3.87×10^5 mN/m. The forces between cadherin on 25:75 DSIDA:DSPC membranes were measured with a soft spring constant of 9.05×10^4 mN/m. Similarly, forces between cadherin immobilized on 100 mol% DSIDA monolayers were measured using both a soft ($k = 3.87 \times 10^5$ mN/m) and a stiff ($k = 1.71 \times 10^6$ mN/m) spring.

Analysis of protein unbinding trajectories

The velocity of cadherin detachment was quantified with a video camera (Dage MTI Inc., Michigan City, IN), video recorder (Panasonic AG-7350, Japan), time–date generator (Panasonic, WJ-810), and video micrometer (Colorado Video Inc., Boulder, CO) interfaced with the surface force apparatus. The time-dependent increase in the wavelengths of the interference fringes as the protein monolayers jumped out of contact was recorded in real time with a video camera placed at the spectrometer exit. The rate of change in the wavelengths was converted to the velocity as a function of the bilayer separation.

RESULTS

Surface density of immobilized cadherin

Surface Plasmon Resonance was used to follow the adsorption of cadherin onto the different DSIDA monolayers used in these studies (Table 1). A typical time course for cadherin adsorption is shown in Fig. 2. Upon injection of the protein solution, there is a rapid rise in the apparent amount of bound cadherin. The increase in the signal following the buffer injection is due to both protein adsorption and changes in the refractive index of the bathing medium. The decrease in the signal following the injection of buffer lacking protein is due to the washout of nonspecifically adsorbed protein and a return of the bulk refractive index of the buffer to its initial value. The limiting final value is used to estimate the equilibrium amount of bound cadherin.

The cadherin surface densities were quantified by determining the amount of radioactively labeled protein bound to

TABLE 1 Locations of attractive minima and strength of adhesion as a function of the cadherin coverage

Mole Fraction of Cu-DSIDA	Surface Density Cadherin/μm^2	Spring Constant (mN/m)	First Minimum (Å)	Adhesion (mN/m)	Second Minimum (Å)	Adhesion (mN/m)	Third Minimum (Å)	Adhesion (mN/m)
25%	1.95×10^4	0.91×10^5	251 ± 3	-0.5 ± 0.2	317 ± 8	-0.3 ± 0.1	393 ± 10	-0.3 ± 0.2
25%*	3.10×10^3	3.87×10^5	255 ± 10	-0.5 ± 0.2	320 ± 10	-0.3 ± 0.2	—	—
40%*	5.62×10^3	3.87×10^5	260 ± 10	-0.9 ± 0.1	n.d.	n.d.	n.d.	n.d.
100%	3.94×10^4	17.10×10^5	259 ± 6	-9 ± 2	334 ± 7	-7 ± 2	398 ± 8	-3 ± 1
100%	3.94×10^4	3.87×10^5	256 ± 5	-9 ± 2	330 ± 10	-6.9 ± 0.7	405 ± 10	-3 ± 1

n.d.: Not determined.
*Measurements with DSIDA in a fluid DTPC lipid matrix, from Sivasankar et al. (1999).

the membranes. The cadherin coverage on membranes containing gel phase DSPC and 25 or 100 mol% DSIDA were, respectively, 1.95×10^4 cadherin/μm^2 and 3.94×10^4 cadherin/μm^2 (Table 1). In studies done with 25 or 40 mol% DSIDA in a fluid DTPC matrix (Sivasankar et al., 1999), the cadherin densities were 5.4×10^3 and 1.0×10^4, respectively. These results were based on the results of four independent measurements for each membrane composition. Although the fluid DTPC lipid allows for lateral cadherin mobility, the binding efficiency of the DSIDA lipid appears to decrease in a fluid lipid matrix.

Definition of the intersurface separation distance at which $D = 0$

In measurements of the normalized force versus the separation distance between identical cadherin monolayers, the distance D is the separation between the surfaces of the supporting lipid bilayers (Fig. 1). The intersurface distance D was determined in two ways. In the first approach, we determined the change in total thickness T_1 (Fig. 1) of the molecular assembly between the crystalline DPPE monolayers after depositing the DSIDA/DSPC monolayer and the immobilization of protein. Thus $D = T_1 - 2 \times T_{DSIDA}$, where T_{DSIDA} is the thickness of the DSIDA monolayer. The cadherin thickness was then determined from the distance D at the onset of the repulsive force between the protein and a bare lipid or between two dilute cadherin monolayers. In the second approach, the thickness of the organic layers between the mica substrates T_2 (Fig. 1) was determined. After draining the apparatus of buffer solution, the surfaces were rinsed with de-ionized water, and all organic layers were removed by ultraviolet irradiation. Thus, the membrane–membrane separation $D = T_2 - 2 \times (T_{DPPE} + T_{DSIDA})$, where T_{DPPE} is the thickness of the DPPE monolayer. The 25-Å thickness of a DPPE film and the 32-Å thickness of a DSIDA monolayer were determined in independent measurements, and have also been reported elsewhere (Marra and Israelachvili, 1985; Sivasankar et al., 1999). Thus, because the bilayer thickness is determined independently and either T_1 or T_2 are measured directly in every experiment, $D = 0$, and hence the intersurface distance, is determined unambiguously. The measured interbilayer distance allows the determination of both the thickness of the cadherin monolayers and their extent of interdigitation.

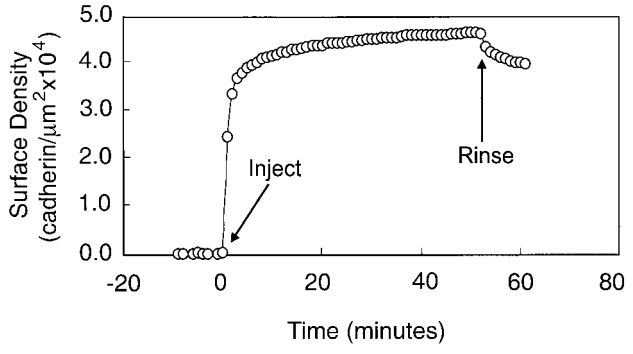

FIGURE 2. Cadherin adsorption time course determined by surface plasmon resonance. The figure shows the adsorption time course in terms of the surface density of cadherin (cadherin/μm^2). After the injection of the protein solution into the flow cell, an initial rise in the signal indicates protein binding. After the signal equilibrated, the flow cell was rinsed with buffer lacking protein. The final total change in the signal indicates the total amount of cadherin bound specifically to the membranes.

Cadherin extracellular domains bind in three different relative alignments

Figure 3 shows the force profiles measured on both approach and separation of cadherin monolayers at the relatively low surface density of 1.95×10^4 cadherin/μm^2 and with a spring constant $k = 9.05 \times 10^4$ mN/m. As D decreases, there is no force between the dilute protein films at $D > 250$ Å (Sivasankar et al., 1999) (Fig. 3 *a*). Due to the 230-Å linear dimension of the cadherin extra-cellular region and the estimated 10-Å length of the iduronic acid spacer (Sivasankar et al., 1999), the proteins interdigitate completely at $D = 250$ Å (Fig. 3 *b*). At $D < 250$ Å, we observe the onset of steric repulsion between the protein and the opposing bilayer surface.

Upon separating the surfaces, we measured an adhesive minimum at an intersurface distance $D = 251 \pm 3$ Å (Table 1) (Fig. 3 *a*). The location of the energy minimum indicates

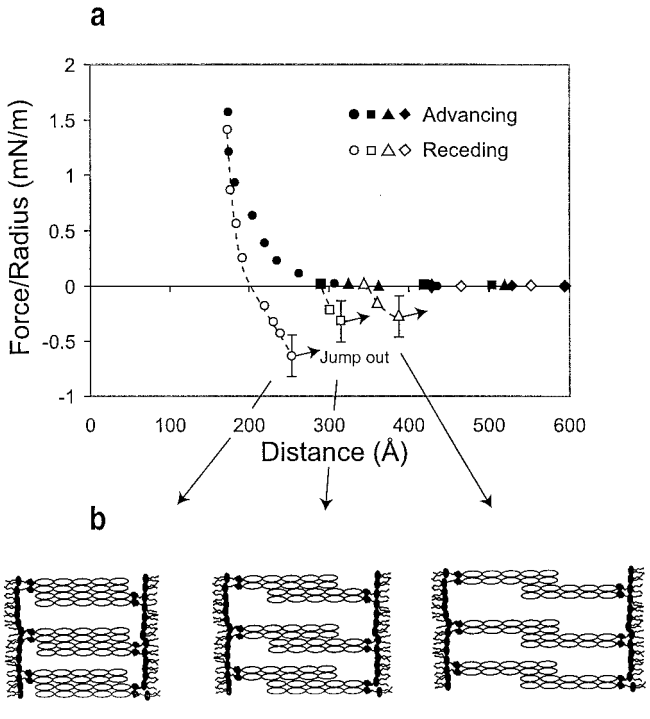

FIGURE 3 (*a*) Normalized force versus distance profile between cadherin monolayers at 1.95×10^4 cadherin/μm^2. Experimental conditions are given in the text. The spring constant $k = 9.05 \times 10^4$ mN/m. Filled symbols indicate the force curves measured on approach, whereas the open symbols show the receding force profiles. The dashed lines are merely to guide the eye. The outward-directed arrows indicate the bilayer distances at which the cadherin bonds rupture, and the proteins jump apart. (*b*) Illustration of the proposed relative cadherin alignments at the positions of the three attractive minima.

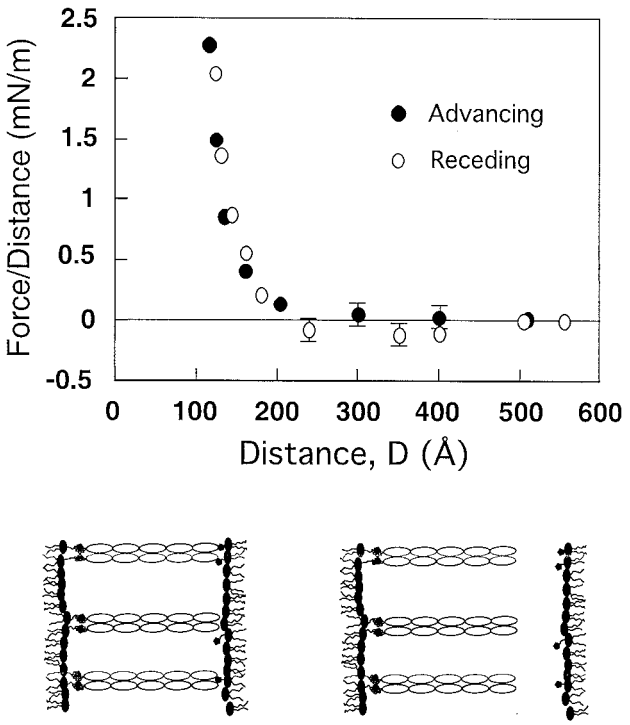

FIGURE 4 Normalized force versus distance curves measured between oriented cadherin (1.95×10^4 cadherin/μm^2) and a bare 25 mol% DSIDA membrane. The normalized force–distance curves measured on approach (*filled symbols*) and separation (*open symbols*) are completely repulsive and reversible. Experimental conditions are described in the text.

that the cadherin ectodomains are completely interdigitated. The strength of adhesion between the cadherin monolayers was -0.5 ± 0.2 mN/m (Table 1). Although we cannot identify the specific domain(s) involved, the attraction is attributed to binding between the completely interdigitated, antiparallel cadherin EC domains (Fig. 3 *b*).

Control experiments confirmed that the adhesion at 251 ± 3 Å was due to the formation of interprotein bonds and not to adhesion between the histidine on the amino-terminal domain and free IDA groups on the opposing bilayer. To show this, we measured the normalized force–distance profile between a cadherin monolayer and a bare 25 mol% DSIDA membrane (Fig. 4.). The cadherin was bound to the lipid bilayers in the absence of calcium. This would prevent any cadherin from binding as an antiparallel adhesive dimer. If the latter occurred, then the exposed histidine tags of some of the proteins could adhere to the opposing membrane. Before the measurements, calcium was re-added to the buffer bathing the sample to reactivate the protein. The force profiles measured between cadherin and the bare membrane during both approach and separation were reversible, and exhibited no adhesion (Fig. 4). There was no force at $D > 250$ Å, and the repulsion at $D < 250$ Å was due to steric repulsion between the protein and the opposing bilayer. The range of the repulsive force confirms both that the repulsion between protein monolayers in Fig. 3 is due to protein–bilayer repulsion, and that the cadherin is oriented end-on. The 230-Å steric thickness of the cadherin ectodomain, determined from the range of the repulsion, agrees with the length estimated from x-ray structures and electron micrographs (Nagar et al., 1996; Pokutta et al., 1994).

To test whether cadherin also binds through other relative alignments, i.e., through the N-terminal domains, we probed for additional binding interactions at different degrees of protein interdigitation. To do this, we controlled the degree of protein overlap by varying the interbilayer spacing D (Fig. 3). For example, at the surface density of 1.95×10^4 cadherin/μm^2, the interbilayer separation between cadherin monolayers was reduced to $D = 430$ Å, and then the proteins were separated (Fig. 3). In the absence of adhesion, the forward and the reverse force profiles were identical (*diamonds*). The formation of adhesive bonds caused a negative deviation in the receding force profile, and the surfaces jumped out of contact from the position of the energy minimum (maximum attraction).

This approach initially identified a second minimum at $D = 320 \pm 10$ Å, and the adhesion was -0.3 ± 0.1 mN/m

at 1.95×10^4 cadherin/μm^2 (Table 1). This second minimum could explain the slowed movement of the bilayers from 260 to 320 Å, if the proteins were being caught in the second minimum after the bonds at 260 Å failed. The adhesion at 320 Å could not, however, account for the full 150-Å range of the sluggish unbinding.

The formation of an additional bond at $D > 320$ Å was not detected at the modest spring constants and protein densities used previously (Sivasankar et al., 1999). To locate other binding orientations, in this study, we increased the signal-to-noise ratio by reducing the force constant of the measuring spring and by increasing the cadherin coverage. The softer spring allowed us to identify weaker bonds between cadherin.

At the highest achievable cadherin surface density (with these bilayers) of 3.94×10^4 cadherin/μm^2 and a force constant of $k = 1.71 \times 10^6$ mN/m, we measured binding at three separations (Fig. 5). On approach, the longer range repulsion at $D < 400$ Å, is due to steric and osmotic forces between the crowded protein layers (Fig. 5 *a*). As expected, the repulsion is larger than that observed between less dense cadherin monolayers. The minimum in the receding force curve at $D = 259 \pm 6$ Å agrees with the measurements at lower coverages (Table 1 and Fig. 5 *A*). The adhesion at the primary minimum is -9 ± 2 mN/m. Between 280 and 400 Å, we measured two additional adhesive minima. The second was at 334 ± 7 Å and the adhesion was -7 ± 2 mN/m (Table 1 and Fig. 5 *A*). The position of the latter site of adhesion is, within the limits of error, identical to the findings at lower cadherin densities. We detected a third adhesive alignment at 398 ± 8 Å, and the attractive force was -3 ± 1 mN/m (Table 1 and Fig. 5 *A*). Only these three minima at 256 ± 5 Å, 330 ± 10 Å, and 400 ± 10 Å were observed with the dense cadherin layers when the stiffness of the measuring spring was reduced to 3.87×10^5 mN/m (data not shown). Reducing the spring constant to 9.05×10^4 mN/m did enable us to detect the third binding alignment at 390 ± 10 Å with 1.95×10^4 cadherin/μm^2 (Fig. 3 *a*). No additional minima were detected between dilute cadherin monolayers with the softer spring. Thus, there are only three sites of adhesion, and their locations are independent of both the transducer stiffness and the protein surface density. These findings are summarized in Table 1.

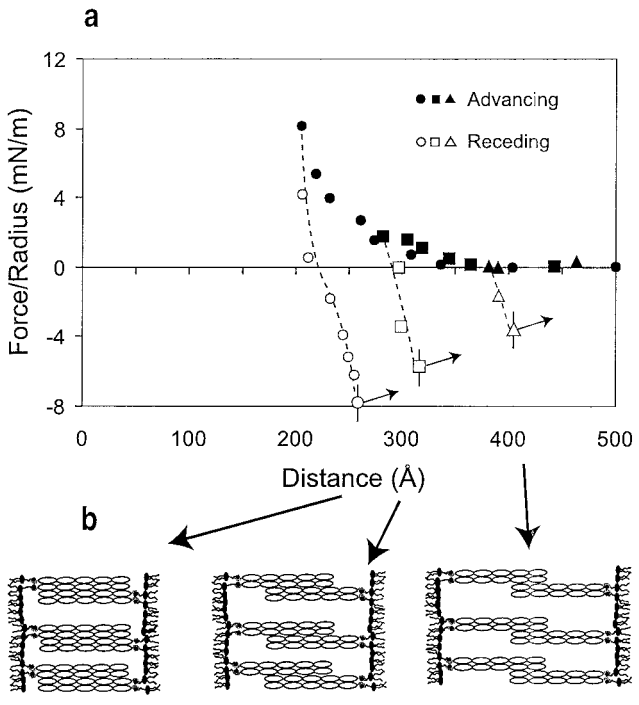

FIGURE 5 (*a*) Normalized versus distance profiles showing the three measured energy minima between cadherin monolayers at a surface density of 3.94×10^4 cadherin/μm^2. The spring constant $k = 1.71 \times 10^6$ mN/m. Filled symbols indicate the force curves measured during approach, whereas open symbols show the receding force profiles. The dashed lines are merely to guide the eye. The different symbols correspond to different measurements in which the proteins were allowed to interact at different bilayer distances before they were separated. (*b*) The proposed protein alignments at the positions of the three attractive force minima.

Cadherin unbinding dynamics

One consequence of these multiple binding alignments is the sluggish detachment of the protein monolayers upon failure of the interprotein bonds at ~250 Å (Sivasankar et al., 1999). Typically, receptor–ligand bond rupture causes the surfaces to abruptly snap out of contact from the position of bond failure (Leckband et al., 1994, 1995b; Moy et al., 1994). However, the detachment of dense cadherin layers is unusual in that unbinding occurs relatively slowly in what appeared to be three distinct stages (Sivasankar et al., 1999).

To quantitatively analyze the dynamics of the cadherin unbinding, we used a video camera and timer to record the time-dependent changes in the interference fringes as the proteins jumped out of contact. Frame-by-frame analysis of the changes in the interference fringe wavelengths gave the interbilayer separation as a function of time. From these data, we determined the detachment velocity as a function of the bilayer separation, and hence of the degree of protein–protein overlap. The velocity–distance trace in Fig. 6 *a* clearly shows that cadherin unbinding occurs in three quantitatively distinct stages (Fig. 6 *a*). In the first regime, following the initial rupture of the primary adhesive complex, the membranes slowly move from 250 ± 10 Å to 330 ± 20 Å at an average velocity of 0.1 ± 0.05 Å/s. In the second regime, which commences at 320 ± 20 Å, the detachment velocity increases gradually from 0.1 ± 0.05 Å/s to 1.0 ± 0.5 Å/s. In the third stage, the surfaces abruptly snap out of contact at $D = 400 \pm 10$ Å. Thus, after the first bonds break at 250 Å, the cadherin is apparently caught in the second minimum, and this impedes the detachment. Near 320 Å, the velocity increases, presumably because the third, weaker minimum is less effective at retarding the cadherin pull-off.

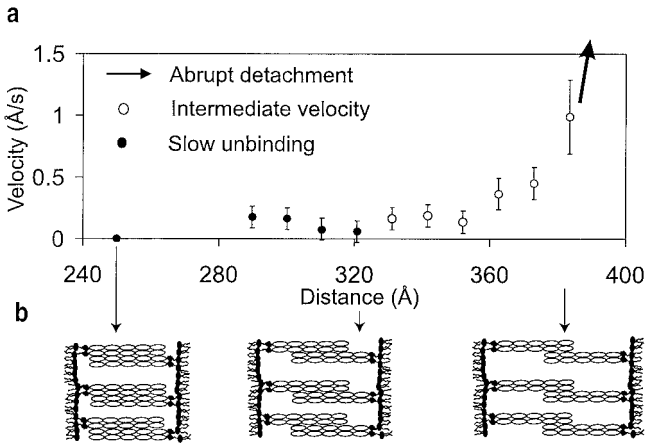

FIGURE 6 (*a*) The measured rate of detachment of cadherin monolayers as a function of the interbilayer distance (3.94×10^4 cadherin/μm^2). (*b*) The proposed protein orientations at the positions of transition between the three distinct stages.

Finally, the proteins abruptly snap out of contact from the third adhesive minimum (Fig. 6 *b*).

This detachment behavior can potentially arise from three different mechanisms: namely, 1) adhesion at multiple sites along the protein unbinding pathway, 2) the restricted fluid flow into the gap between the curved surfaces due to the surface-anchored protein (Klein, 1983), or 3) frictional drag between antiparallel cadherin rods. We confirmed the presence of multiple adhesive minima along the unbinding trajectory. Previous calculations also showed that the frictional drag on the proteins as they slide past each other is negligible at the measured velocities (Sivasankar et al., 1999). Finally, Appendix A describes calculations of the hydrodynamic drag resulting from the flow of solvent into the narrow gap formed during surface separation. Although this dissipative force is enhanced by the presence of the oriented, rod-like protein ectodomains, which are an additional source of hydrodynamic friction, the drag is negligible at the detachment velocities observed in these studies. The slow unbinding is, therefore, due to the rupture and formation of successive bonds along the unbinding path.

DISCUSSION

These direct-force measurements suggest that, instead of binding in a single unique orientation, cadherins bind in three distinct adhesive alignments. These alignments at the interbilayer separations of 250, 320, and 400 Å were identified from the locations of the corresponding minima in the measured energy–distance profiles (Figs. 3 and 5). The strongest binding interaction occurs when the proteins are completely interdigitated. A second adhesive alignment is at a distance where the interdigitated proteins are separated by 1.5 ± 0.5 EC domains. Finally, the third adhesive contact at 400 ± 10 Å corresponds approximately to the overlap between the outer two domains (CEC1–2) of each protein. Unfortunately, we could not obtain more precise measurements of the locations of the outer two minima. The ± 10 Å error is not due to the uncertainty in the distance measurement technique. It is because of the difficulty in identifying the exact distance at which the protein bonds fail and the opposing proteins begin to slowly move apart. The latter determination is particularly difficult at high cadherin densities where the detachment is very slow.

These data contradict previous assumptions about the importance of the direct interactions between the N-terminal domains in cadherin-mediated adhesion because the strongest adhesion is between completely interdigitated, antiparallel EC domains. Because the N-terminal domain is in potential contact with the opposing protein in each measured antiparallel binding alignment, the data are nevertheless consistent with data implicating the N-terminal domains in tissue specificity. The additional binding configurations at $D < 400$ Å could not have been identified in the crystal structures because only EC1 and EC1–2 were crystallized. Similar interdigitated cadherin configurations were not observed in electron micrographs of pentamers of chimeras E-cadherin and the cartilage oligomeric matrix protein. The splay between adjacent cadherins imposed by the formation of the pentamers may inhibit this. Alternatively, the presentation of the proteins may impede lateral interactions that could affect binding at the high densities on the cell surface. In qualitative agreement with the observations of Tomschy et al. (1996), the bonds formed when the CEC1–2 segments of CEC1–5 overlap are weak. However, the range of this attraction is inconsistent with the end-on N-terminal domain interactions proposed by Shapiro et al. (1995).

Because the oriented protein monolayers are confined to the surfaces of hemicylindrical silica lenses oriented perpendicular to each other, it is reasonable to address the issue of how the curved surfaces might affect the measured force–distance profile. First, the SFA measures the total force between the two surfaces, integrated over the entire region of the interaction. In the experiments, the radius of curvature of the supporting crossed-cylinders is $R = 1.5$–2 cm, whereas the range of the molecular interactions relevant to this study is <50 nm. Thus, the local regions of the interacting surfaces are essentially flat on a molecular scale, so that the domain registry of adjacent and/or antiparallel proteins differs by less than 2 Å over a radial distance of ~ 1 micron, i.e., within a 3 μm^2 area. The net force between curved surfaces $F_c(D)$, determined by integrating the force between these locally flat patches over the entire surface, is directly proportional to the energy per area between two equivalent flat surfaces $E_f(D)$: $F_c(D) = 2\pi R E_f(D)$ (Israelachvili, 1992b). Here, R is the geometric average radius of the cylinders. The latter relationship is the Derjaguin approximation, and is derived in several textbooks (Hunter, 1989; Israelachvili, 1992b; Russell et al., 1989). It is valid

for radii $R \gg D$, where D is the range of the force. The non-intuitive consequence of this is that curvature does not smear out the discrete peaks and valleys in the interaction potential between two flat surfaces exposing molecules, which interact via an oscillatory potential. Our exact numerical calculations (Appendix B) reconfirm that this relationship holds for oscillatory potentials for $R > 1$ micron. Therefore the minima in the force–distance curve between the crossed cylinders correspond with the positions of maximum attraction between identical proteins on opposed flat plates.

Importantly, oscillatory or periodic forces have been measured with the SFA in several different systems (Israelachvili, 1992a, 1987; Israelachvili and Kott, 1988; Israelachvili and Pashley, 1983; Horn and Israelachvili, 1981, 1988; Christenson and Horn, 1983; Christenson and Israelachvili, 1984; Christenson, 1985; Leckband et al., 1994; Kekicheff et al., 1990). These oscillations also extended up to 20 nm in a few cases. In several of those reports, the surface force measurements confirmed the theoretically predicted oscillations in the intersurface potentials between two flat plates (Israelachvili, 1987). Moreover the periods of the oscillations corresponded to the dimensions of the molecules confined between the surfaces (Israelachvili and Pashley, 1983; Horn and Israelachvili, 1981, 1988; Christenson et al., 1987; Christenson, 1985; Christenson and Israelachvili, 1984; Christenson and Horn, 1983; Kekicheff et al., 1990; Leckband et al., 1994).

In surface force measurements of other receptor–ligand interactions, the distance dependence of the measured adhesion between the cytochrome c/cytochrome b5, streptavidin/biotin, CD2/CD48, and Fab′/fluorescein pairs were within 3 Å of the predicted distances based on the crystallographically determined protein structures (Helm et al., 1991; Leckband et al., 1994, 1995a,b; Yeung and Leckband, 1997; Yeung et al., 1999). The latter protein dimensions ranged from 3 to 7 nm, which are only 3–10-fold smaller than cadherin. In some cases, the proteins were bound by long (2.7 nm) tethers. In every instance, upon bond failure, the proteins and ligands abruptly jumped out of contact from a single intersurface separation. On a molecular length scale, the substrate curvature $1/R = ½$ cm $(= 50\ m^{-1})$ will have a similarly negligible impact on a 7 nm $(1/D \sim 10^8 m^{-1})$ interaction as on a 25–40-nm interaction $(1/D \sim 10^7 m^{-1})$. As discussed above, the negligible effect of surface geometry on the positions of the minima in the oscillatory intersurface energy–distance curves has been demonstrated both experimentally and theoretically. The spatially distinct minima reported in this study, therefore, reflect the different protein alignments in which cadherin binds (cf. Appendix B).

We propose that these multiple cadherin binding configurations may function as "brakes" to slow the abrupt failure of cadherin junctions. In particular, the positions of the three transitions in the velocity–distance profiles in Fig. 6 *a* correspond to each of the three minima in the interaction profile (Fig. 6 *b*). The impeded detachment of the adherent cadherin monolayers appears to be due to the successive rupture and formation of bonds as the proteins slide past each other. The multiple minima along the unbinding pathway of cadherin, therefore, appear to serve as catches that prevent the abrupt failure of the cadherin cross-bridges.

To our knowledge, there are only two reports of a similar sluggish jump-out from an adhesive minimum. The very slow (100 s) pull-off of adsorbed polymers was attributed to the hydrodynamic drag caused by the fluid flow through the dense polymer layers (Klein, 1983). Flexible polymers can form highly entangled networks (de Gennes, 1988), but the hydrodynamic friction between oriented, relatively stiff rods is significantly lower. Our calculations (Appendix A) show that the lubrication force between the interdigitated protein layers has no effect on the protein detachment. Another study of the separation of Protein A-coated mica surfaces found that separation occurs in two stages with jump-out times ranging from 1 to 5 s. This multiple stage rupture was attributed to the formation of nonspecific adhesive bridges between either Protein A and the opposing mica surface or between Protein A molecules on opposing surfaces (Ohnishi et al., 1998). In our experiments however, the absence of adhesion between a cadherin monolayer and an opposing bare DSIDA membrane rules out the involvement of such bridging interactions.

Although the positions of the adhesive minima are independent of the cadherin density and the force constant of the spring, the adhesion (depth of the minimum) does increase with the amount of protein on the membranes. At the primary minimum, with cadherin layers on gel phase lipids at surface densities of 1.95×10^4 cadherin/μm^2, the adhesion was -0.5 ± 0.3 mN/m. An increase in the cadherin density to 3.9×10^4 cadherin/μm^2 increased the adhesion to -9 ± 2 mN/m. The adhesion is related to the energy per area between deformable materials by $F/R = 1.5\pi E$ (Johnson et al., 1971; Israelachvili, 1992b). The estimated average energy per cadherin bound to the gel phase membranes would be ~1 kT at 1.95×10^4 cadherin/μm^2 and 12 kT at 3.94×10^4 cadherin/μm^2. This increase may be due, in part, to density-dependent lateral association between proteins (Brieher et al., 1996) and to the higher probability of binding between the denser protein monolayers. Consistent with the latter argument, the bond energy estimated from the adhesion between proteins on fluid–lipid membranes, which consisted of 25:75 and 40:60 DSIDA:DTPC mixtures, was 4–5 kT (Sivasankar et al., 1999). In the latter case, the proteins could move relatively freely over the surface. All of these values are lower than those measured in conjunction with the extraction of lipid anchors from the membrane (Leckband et al., 1995a), or with the rupture of antibody–antigen bonds (Leckband et al., 1995b). However, these bond energies are only estimates because 1) the dynamic binding and unbinding make it difficult to determine the

absolute numbers of proteins that are involved in adhesion (Saterbak and Lauffenburger, 1996; Seifert, 2000; Vijayendran et al. 1998) and 2) it is difficult to determine the number of opposing proteins in register at the time of the measurement (Leckband et al., 1995a). The main points are that the adhesion increases with the number of proteins on the membranes, and, most importantly, that the positions of the adhesive minima are independent of both the protein densities and the lateral mobility of the cadherin.

In summary, these direct measurements of the adhesion between the EC segments of C-cadherin as a function of the relative protein separation show that the proteins bind in three distinct antiparallel alignments. These adhesive alignments correspond to the velocity transitions along the protein unbinding trajectory. The data suggest that, upon failure of the bonds at the primary minimum, the additional minima along the unbinding trajectory serve as traps or catches, which retard cadherin detachment. This built-in catch-mechanism prevents sudden adhesive failure, and may function to stabilize cadherin junctions between cells.

APPENDIX A

The lubrication force between two surfaces coated with rigid rods is given by (Fredrickson and Pincus, 1991)

$$F_{\mathrm{H}} = \frac{-6\pi R^2 \eta V}{h - 2L}, \tag{A1}$$

where R is the radius of curvature of the surface, η is the bulk solvent viscosity, V is the detachment velocity, h is the intersurface separation distance, and L is the length of the rods. When the rods are completely interdigitated, the hydrodynamic force is given by the scaling expression (Fredrickson and Pincus, 1991; Rabin et al., 1991),

$$F_{\mathrm{H}} = -\pi\eta V R^2 \int_{\mathrm{h}}^{2\mathrm{L}} \frac{h' - h}{h'\xi(h')^2}\,\mathrm{d}h'. \tag{A2}$$

Here $\xi(h')$ is the hydrodynamic screening length. Unlike flexible polymers in good solvents that interdiffuse at contact to form entangled networks (de Gennes, 1988), the cadherin monolayers resemble a dilute solution of oriented rods. The hydrodynamic screening length for a suspension of stiff, slender rods of length L and diameter d is given by $\xi(h') = d|\mathrm{Log}\ \phi/\phi|^{1/2}$, where ϕ is the volume fraction of the rods (Shaqfeh and Fredrickson, 1990). If the ectodomains are spaced a distance S apart, then,

$$\xi(h') = d\left|\frac{\mathrm{Log}(2d^2/h's^2)}{2Ld^2/h's^2}\right|. \tag{A3}$$

The time required to jump out from the primary adhesive minimum can then be calculated, using a simple force balance between the hydrodynamic force F_{H}, the surface force F_{S}, and the restoring force of the cantilever spring F_{k}: $F_{\mathrm{H}} + F_{\mathrm{S}} = F_{\mathrm{k}}$ (Klein, 1983). As the surfaces jump out from the first minimum at $h1$ to a distance $h2$, it can be shown that the time τ required to traverse the $2L$ distance to the ends of the ectodomains is

$$\tau = \pi\eta R^2 \int_{\mathrm{h1}}^{\mathrm{h2}} \frac{\int_{\mathrm{h}}^{2\mathrm{L}} (h' - h)/h'\xi(h')^2)\mathrm{d}h'}{F_{\mathrm{s}} - F_{\mathrm{k}}}\,\mathrm{d}h. \tag{A4}$$

From Eqs. 3 and 5, the detachment time in the nonoverlapping region ($h > 2L$) is

$$\tau = \int_{\mathrm{h1}}^{\mathrm{h2}} \frac{6\pi R^2 \eta}{(h - 2L)(F_{\mathrm{s}} - F_{\mathrm{k}})}\,\mathrm{d}h. \tag{A5}$$

We calculated the effect of hydrodynamic drag on the detachment of cadherin monolayers at a surface density of 3.94×10^4 cadherin/μm^2. An oscillatory function with minima at 250, 320, and 400 Å represented the intersurface force F_{s}. The restoring force was given by the deflection of the spring multiplied by the spring constant. With the dimensions of the cadherin EC domain (Nagar et al., 1996; Pertz et al., 1999; Pokutta et al., 1994; Shapiro et al., 1995) and experimental values for the radius, protein surface density, and spring constant from our measurements, the calculated detachment time is ~1 s. This is much shorter than the experimentally measured 10.5 min, and shows that the lubrication force has an insignificant effect on cadherin detachment.

APPENDIX B: NUMERICAL CALCULATIONS OF THE FORCE–DISTANCE PROFILE BETWEEN TWO SURFACES INTERACTING THROUGH AN OSCILLATORY POTENTIAL

We investigated the effect of the crossed-cylinder geometry on the measured normalized force–distance profiles between two surfaces interacting through an oscillatory potential. To do this, we used the surface element integration method (Battacharjee and Elimelech, 1997) to calculate the exact force F_{SEI} between a sphere and flat plate in terms of the interaction energy per unit area $E(D)$ between two flat plates of identical composition separated by a distance D. An oscillatory function, which exhibited attractive minima at the same locations as those measured with the force apparatus, was used to describe the distance dependence of the local interaction energy per area between the opposing parallel plates.

With the surface element integration method, one calculates the exact interaction energy between a sphere and a flat surface for any arbitrary one-dimensional, interaction potential $E(h)$ per area:

$$U_{\mathrm{SEI}}(D) = 2\pi \int_0^{\mathrm{R}} E\left(D + R - R\sqrt{1 - \frac{a^2}{R^2}}\right) a\,\mathrm{d}a$$

$$-2\pi \int_0^{\mathrm{R}} E\left(D + R + R\sqrt{1 - \frac{a^2}{R^2}}\right) a\,\mathrm{d}a. \tag{B1}$$

Here, R is the radius of the sphere, and D is the closest distance between the sphere and the plane. The above integrals were evaluated by numerical integration with values of D ranging from 240 to 440 Å in 0.5-Å steps. The net energy U_{SEI} between the sphere and a flat plate at each distance $D + \Delta D/2$ was calculated from the relation $F_{\mathrm{SEI}} = -\Delta U_{\mathrm{SEI}}/\Delta D$, where $\Delta D = D_{(\mathrm{i}+1)} - D_{(\mathrm{i})}$ and $\Delta U_{\mathrm{SEI}} = U_{\mathrm{SEI}(\mathrm{i}+1)} - U_{\mathrm{SEI}(\mathrm{i})}$.

To compare the exact surface element integration results with the Derjaguin Approximation (DA), which assumes that curvature effects are negligible for large radii, we also used the approximation to calculate the energy between a sphere and flat plate (Hunter, 1989; Israelachvili, 1992b). This gives the interaction energy U_{DA} between a sphere and flat plate in terms of energy per area between equivalent flat surfaces (Hunter, 1989):

$$U_{\mathrm{DA}}(D) = 2\pi R \int_{\mathrm{D}}^{\infty} E(h)\,\mathrm{d}h. \tag{B2}$$

Here, h is the distance between the two flat planes, and D is the closest distance between the sphere and the plane. Recall that $F_{DA}(D) = -dU_{DA}/dU = 2\pi RE(D)$. The above integral was also evaluated numerically in 0.5-Å steps between 240 and 440 Å. $E(h)$ was a polynomial function with coefficients chosen to yield three minima at $D = 250$, 330, and 400 Å. This exhibits the periodicity of the adhesive minima over the same range of interaction, but is not a measurement of the protein–protein potential.

The surface element integration method (Battacharjee and Elimelech, 1997) was used to calculate the exact energy–distance profile between a sphere of radius 1.5 cm (a typical value of R in SFA experiments) and a flat surface interacting through an oscillatory potential. The exact calculations of the integrated force between the sphere and flat surface reproduced the oscillations in the potential. Moreover, results with the SEI calculations agreed quantitatively with calculations done using the DA (Fig. 7).

We then identified the critical radius below which substrate curvature generates significant deviations in the normalized force profiles relative to the energy–distance curves between two flat surfaces. To do this, we systematically varied the radius R from 100 Å to 1.5 cm in steps of 100 Å, while simultaneously monitoring the change in the shape of the force–distance curve. For radii of curvature $R > 1.0$ μm, the exact surface element integration results quantitatively agreed with those calculated with the DA. Below $R \sim 1$ μm, the attractive potential wells calculated with the DA become shallower and broader (data not shown). Thus, substrate curvature distorts the potential only for spheres with radii below 1 μm, which is four orders of magnitude smaller than used in the surface force measurements. These calculations confirm that the multiple minima observed in our normalized force profiles reflect the protein–protein interactions, and are not distorted by the slight curvature of the underlying substrate.

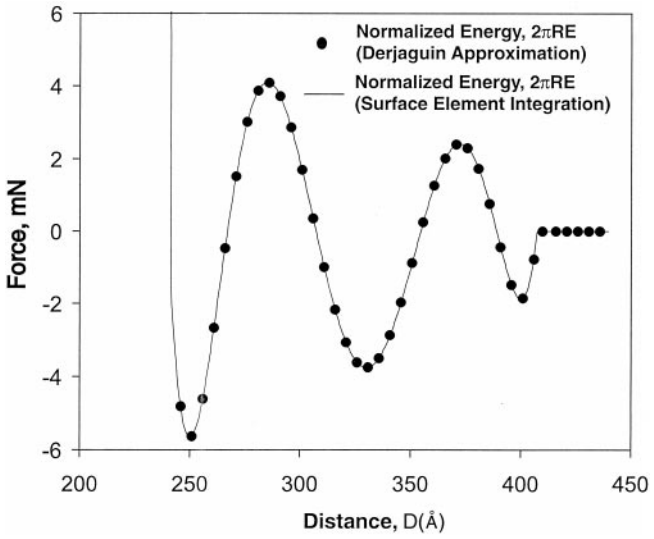

FIGURE 7 The calculated force–distance profiles between a flat surface and a sphere. The materials on the two are assumed to interact through an oscillatory potential. The solid line shows the exact force–distance profile (normalized energy) for the sphere–flat interaction calculated by surface element integration as described in Appendix B. The filled circles show the normalized energy–distance profile between the same two surfaces calculated with the DA. In the latter case, the energy distance profile was calculated between two flat surfaces, and then normalized by $2\pi R$. These results show that, for large R, the exact calculations agree quantitatively with the DA, and thereby confirm the relationship between the integrated force between the hemicylinders and the potential between two flats.

REFERENCES

Battacharjee, S., and M. Elimelech. 1997. Surface element integration—a novel technique for evaluation of DLVO interaction between a particle and a flat plate. *J. Coll. Int. Sci.* 193:273–285.

Brieher, W. M., A. S. Yap, and B. M. Gumbiner. 1996. Lateral dimerization is required for the homophilic binding activity of C-cadherin. *J. Cell Biol.* 135:487–496.

Christenson, H. 1985. Forces between solid surfaces in a binary mixture of non-polar liquids. *Chem. Phys. Lett.* 118:455–458.

Christenson, H., D. W. R. Gruen, R. G. Horn, and J. N. Israelachvili. 1987. Structuring in liquid alkanes between solid surfaces: force measurements and mean-field theory. *J. Chem. Phys.* 87:1834–1841.

Christenson, H., and R. G. Horn. 1983. Direct measurement of the force between solid surfaces in a polar liquid. *Chem. Phys. Lett.* 98:45–48.

Christenson, H., and J. N. Israelachvili. 1984. Temperature dependence of solvation forces. *J. Chem. Phys.* 80:4566–4567.

de Gennes, P. 1988. Scaling Concepts in Polymer Physics. Cornell University Press, Ithaca, NY.

Fredrickson, G., and P. Pincus. 1991. Drainage of compressed polymer layers: dynamics of a "squeezed sponge." *Langmuir.* 7:786–795.

Gumbiner, B. M. 1996. Cell adhesion: the molecular basis of tissue architecture and morphogenesis. *Cell.* 84:345–357.

Helm, C. A., W. Knoll, and J. N. Israelachvili. 1991. Measurement of ligand–receptor interactions. *Proc. Natl. Acad. Sci. U.S.A.* 88: 8169–8173.

Horn, R., and J. N. Israelachvili. 1981. Direct measurement of structural forces between two surfaces in a nonpolar liquid. *J. Chem. Phys.* 75: 1400–1411.

Horn, R., and J. N. Israelachvili. 1988. Molecular organization and viscosity of a thin film of molten polymer between two surfaces as probed by force measurements. *Macromolecules.* 21:2836–2841.

Hunter, R. 1989. Foundations of Colloid Science. Oxford University Press, Oxford, UK. 191–194.

Israelachvili, J. 1973. Thin film studies using multiple-beam interferometry. *J. Coll. Int. Sci.* 44:259–272.

Israelachvili, J. 1987. Solvation forces and liquid structure, as probed by direct force measurements. *Acc. Chem. Res.* 20:415–421.

Israelachvili, J. 1992a. Adhesion forces between surfaces in liquids and condensable vapours. *Surf. Sci. Rep.* 14:110–159.

Israelachvili, J. 1992b. Intermolecular and Surface Forces. Academic Press, New York. 155–159.

Israelachvili, J., and G. E. Adams. 1978. Measurement of forces between two mica surfaces in aqueous electrolyte solutions in the range 0–100 nm. *J. Chem. Soc. Faraday Trans. I.* 74:975–1001.

Israelachvili, J., and S. J. Kott. 1988. Liquid structuring at solid interfaces as probed by direct force measurements: the transition from simple to complex liquids and polymer fluids. *J. Chem. Phys.* 88:7162–7166.

Israelachvili, J., and P. McGuiggan. 1990. Adhesion and short-range forces between surfaces: new apparatus for surface force measurements. *J. Mater. Res.* 5:2223–2231.

Israelachvili, J., and R. M. Pashley. 1983. Molecular layering of water at surfaces and origin of repulsive hydration forces. *Nature.* 306:249–250.

Johnson, K. L., K. Kendall, and A. D. Roberts. 1971. Surface energy and the contact of elastic solids. *Proc. R. Soc. Lond. A.* 324:301–313.

Kekicheff, P., W. A. Ducker, B. W. Ninham, and M. P. Pileni. 1990. Multilayer adsorption of cytochrome *c* on mica around isoelectric pH. *Langmuir.* 6:1704–1708.

Klein, J. 1983. Forces between mica surfaces bearing adsorbed macromolecules in liquid media. *J. Chem. Soc. Faraday Trans. I.* 79:99–118.

Koch, A., D. Bozic, O. Pertz, and J. Engel. 1999. Homophilic adhesion by cadherins. *Curr. Op. Struct. Biol.* 9:275–281.

Lavrik, N., and D. Leckband. 2000. Optical and direct force measurements of the interaction between monolayers of aromatic macrocycles on surfactant monolayers. *Langmuir.* 16:1842–1851.

Leckband, D. E., T. L. Kuhl, H. K. Wang, W. Müller, and H. Ringsdorf. 1995b. 4-4-20 anti-fluorescyl IgG Fab′ recognition of membrane bound

hapten: direct evidence for the role of protein and interfacial structure. *Biochemistry*. 34:11467–11478.

Leckband, D., W. Müller, F.-J. Schmitt, and H. Ringsdorf. 1995a. Molecular mechanisms determining the strength of receptor-mediated intermembrane adhesion. *Biophys. J.* 69:1162–1169.

Leckband, D., F.-J. Schmitt, J. Israelachvili, and W. Knoll. 1994. Direct force measurements of specific and nonspecific protein interactions. *Biochemistry*. 33:4611–4624.

Marra, J., and J. Israelachvili. 1985. Direct measurements of forces between phosphatidylchlone and phosphatidylethanolamine bilayers in aqueous electrolyte solutions. *Biochemistry*. 24:4608–4618.

Moy, V. T., E.-L. Florin, and H. E. Gaub. 1994. Intermolecular forces and energies between ligands and receptors. *Science.* 266:257–259.

Nagar, B., M. Overduin, M. Ikura, and J. M. Rini. 1996. Structural basis of calcium-induced E-cadherin rigidification and dimerization. *Nature.* 380:360–364.

Nose, A., K. Tsuji, and M. Takeichi. 1990. Localization of specificity determining sites in cadherin cell adhesion molecules. *Cell.* 61:147–155.

Ohnishi, S., M. Murata, and M. Hato. 1998. Correlation between surface morphology and surface forces of protein A adsorbed on mica. *Biophys. J.* 74:455–465.

Pertz, O., A. Bozic, W. Koch, C. Fauser, A. Brancaccio, and J. Engel. 1999. A new crystal structure, Ca^{2+} dependence and mutational analysis reveal molecular details of E-cadherin homoassociation. *EMBO J.* 18: 1738–1747.

Pokutta, S., K. Herrenknecht, R. Kemler, and J. Engel. 1994. Conformational changes of the recombinent extracellular domain of E-cadherin upon calcium binding. *Eur. J. Biochem.* 223:1019–1026.

Rabin, Y., G. H. Fredrickson, and P. Pincus. 1991. Compression of grafted polyelectrolyte layers. *Langmuir*. 7:2428–2430.

Russell, J., D. Saville, and W. Schowalter. 1989. Colloidal Dispersions. Chapt. 5. Cambridge University Press, Cambridge, UK.

Saterbak, A., and D. A. Lauffenburger. 1996. Adhesion mediated by bonds in series. *Biotechnol. Prog.* 12:682–699.

Seifert, U. 2000. Rupture of multiple parallel bonds under dynamic loading. *Phys. Rev. Lett.* 84:2750–2753.

Shapiro, L., A. M. Fannon, P. D. Kwong, A. Thompson, M. G. Lehmann, G. Grübel, J.-F. Legrand, J. Als-Nielsen, D. R. Colman, and W. A. Hendrickson. 1995. Structural basis of cell–cell adhesion of cadherins. *Nature*. 374:327–337.

Shaqfeh, E., and G. H. Fredrickson. 1990. The hydrodynamic stress in a suspension of rods. *Phys. Fluids A.* 2:7–24.

Shnek, D., D. W. Pack, D. Y. Sasaki, and F. H. Arnold. 1994. Specific protein attachment to artificial membranes via coordination to lipid-bound copper (II). *Langmuir*. 10:2382–2388.

Sivasankar, S., W. Brieher, N. Lavrik, B. Gumbiner, and D. Leckband. 1999. Direct molecular force measurements of multiple adhesive interactions between cadherin ectodomains. *Proc. Natl. Acad. Sci. U.S.A.* 96:11820–11824.

Takeichi, M. 1991. Cadherin cell adhesion receptors as a morphogenetic regulator. *Science.* 251:1451–1455.

Takeichi, M. 1993. Cadherins in cancer: implications for invation and metastasis. *Curr. Opin. Cell Biol.* 5:806–811.

Takeichi, M. 1995. Morphogenetic roles of classic cadherins. *Current Opinion in Cell Biology* 7:619–627.

Tamura, K., W.-S. Shan, W. A. Hendrickson, D. R. Colman, and L. Shapiro. 1998. Structure–function analysis of cell adhesion by neural (N-) cadherin. *Neuron.* 20:1153–1163.

Tomschy, A., F. Charlotte, R. Landwehr, and J. Engel. 1996. Homophilic adhesion of E-cadherin occurs by a cooperative two-step interaction of N-terminal domains. *EMBO J.* 15:3507–3514.

Vijayendran, R., D. Hammer, and D. Leckband. 1998. Simulations of the adhesion between molecularly bonded surfaces in direct force measurements. *J. Chem. Phys.* 108:7783–7793.

Vijayendran, R., and D. Leckband. 1999. A computational reaction-diffusion model for the analysis of transport-limited kinetics. *Anal. Chem.* 71:5405–5412.

Weis, W. I. 1995. Cadherin structure: a revealing zipper. *Structure.* 3:425–427.

Yap, A. S., W. M. Brieher, and B. M. Gumbiner. 1997. Molecular and functional analysis of cadherin-based adherens junctions. *Annu. Rev. Cell. Dev. Biol.* 13:119–146.

Yeung, C., and D. Leckband. 1997. Molecular level characterization of microenvironmental influences on the properties of immobilized proteins. *Langmuir.* 13:6746–6754.

Yeung, C., T. Purves, A. Kloss, S. Sligar, and D. Leckband. 1999. Cytochrome c recognition of immobilized, orientational variants of cytochrome b5: direct force and equilibrium binding measurements. *Langmuir.* 15:6829–6836.